

Spectrum of Relaxation Times in GeO_2 Glass

A. Napolitano and P. B. Macedo

Institute for Materials Research, National Bureau of Standards, Washington, D.C. 20234

(April 29, 1968)

Index-of-refraction versus time isotherms have been established for germania glass. Using the crossover technique with air-quenched samples and applying the two relaxation time model previously reported for borosilicate glass, it was found that the width of the spectrum of relaxation times for germania glass was temperature dependent. Upon analyzing this in terms of a distribution of activation energies, the results showed that, similarly to B_2O_3 , activation energies smaller than the activation energy present in the Arrhenius region appear at low temperatures.

Extensive viscosity measurements by the fiber elongation method were made from 10^{11} to 6×10^{14} poises. From this data a lower and more precise value of the activation energy ($E_\eta = 72.3$ kcal/mol) was obtained in the annealing range.

Key Words: Activation energy; annealing; germania glass; index of refraction; relaxation times; thermal expansion; two relaxation model; viscosity.

1. Introduction

In a recent paper [1]¹ a two relaxation model was proposed for obtaining distribution of relaxation times from annealing experiments on a borosilicate crown (BSC) glass [2]. Since this model was only applied to a BSC glass, and there was a remote possibility that this glass was immiscible, it was decided to apply this interpretation to similar annealing experiments performed on a one component glass— GeO_2 .

Another reason for choosing GeO_2 is that the temperature dependence of its viscosity is almost Arrhenius i.e., $\eta = A \exp(E_\eta/RT)$ [3, 4]. A series of papers by Macedo, Litovitz and others [5, 6, 7, and 8] have connected the transition between Arrhenius and non-Arrhenius behavior with the appearance of a distribution of relaxation times. Thus this study of GeO_2 glass might provide further information into the nature of the distribution of relaxation times.

2. Experimental Procedure

2.1. Sample Preparation

The GeO_2 batch² used to make the glass was obtained from the Eagle-Pitcher Company, Semi-Conductor Branch, Miami, Oklahoma. It was specified

as "electronic grade." Spectrographic analysis of the GeO_2 batch revealed faint traces (less than 0.0001%) of Ca, Fe, and Pb and traces (less than 0.001%) of Mg and Si. The detection of Al and Cu was questionable.

The GeO_2 batch was melted in a platinum crucible at 1600 °C and refined overnight at 1500 °C. This produced a seed-free glass. The crucible of molten glass was then quickly cooled to room temperature so that the glass could be removed in several large pieces. These pieces were "fine annealed" (cooled at a relatively slow constant rate through the transformation range). Small samples approximately 1 cm square and 1 mm thick were cut from these large pieces for the annealing experiments. Since GeO_2 glass is hygroscopic, kerosene was used not only in the preparation of these small samples but also for storage at room temperature.

2.2. Refractive Index Measurements

All the index measurements were made at room temperature on the Grauer refractometer [9] using the sodium D line. The GeO_2 glass was found to be still hygroscopic at elevated temperatures in the annealing range and under these conditions a white hydrated film formed on the sample and hampered index measurements. The rate of formation of this film was reduced somewhat by flooding the furnace with dry nitrogen gas during the annealing experiments. Even so, this film quite often slowly formed during the longer annealing experiments and prevented accurate index measurements. In order to

¹ Figures in brackets indicate the literature references at the end of this paper.

² Certain commercial materials are identified in this paper in order to adequately specify the experimental procedure. In no case does such identification imply recommendation or endorsement by the National Bureau of Standards, nor does it imply that the material identified is necessarily the best available for the purpose.

proceed with the heat treatments the edges of each sample had to be repeatedly ground during the tests. It is recalled [2] that the accuracy of the measured index of refraction depends on the angle between edges being 90° or very close to 90° . This continuous regrinding affected this angle and reduced both the accuracy and the precision of the measurements. As a result there is a larger scatter in the GeO_2 index measurements than those previously reported for BSC glass [2].

2.3. Heat Treatment

The annealing procedure used here is the same as that used for the BSC glass [2]. All samples were held at 600°C for $\frac{1}{2}$ hr before quenching from the furnace to room temperature. This determined the starting and equilibrium value of index which was the same for all samples. The special rotating-type furnace was then set at some lower temperature in the transformation range, the samples were inserted into the furnace, held for a given time, one sample was dropped out, and its index measured. Then, the sample was reinserted into the furnace, another sample dropped out at a later time and the process was repeated until a complete time-index (approach) curve for each temperature had been established.

The insertion into the furnace and release of samples (1 to 9) from the furnace at different time intervals was made without disturbing the temperature stability.

3. Results

3.1. Thermal Expansion

In order to find the transformation region (annealing range) the linear thermal expansion of the GeO_2 glass was measured by the interferometric method [10]. The furnace was heated at the rate of 2°C per minute from room temperature through the deformation temperature of the germania sample under test. The resulting linear thermal expansion curve is shown in figure 1 and calculated to be $7.70 \times 10^{-6}/^\circ\text{C}$ between 30 and 400°C . This is in good agreement with Mackenzie [11] and verifies the measurements reported by Dennis and Laubengayer [12]. The deformation point (600°C) and critical point (505°C) roughly denote the limits of the annealing range. The annealing range is where structural equilibrium can be reached within reasonable times and lies in the upper part of the transformation region. The low temperature thermal expansion data shown in figure 1, were reported by Spinner and Cleek [13].

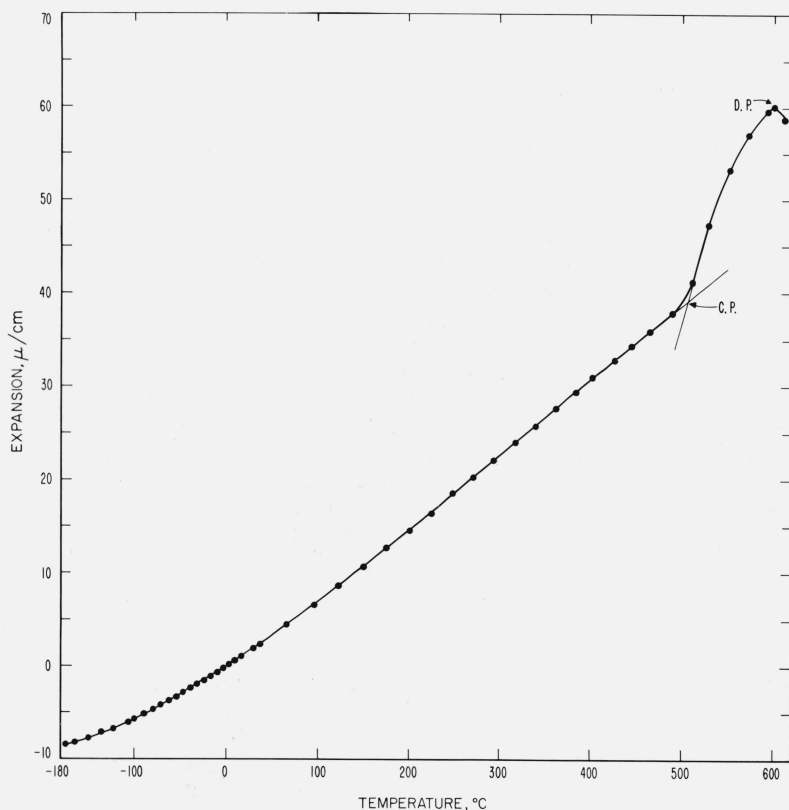


FIGURE 1. Thermal expansion of vitreous GeO_2 showing the critical point and the deformation point.

Data below 30°C from ref. (13).

3.2. Approach Curves

The index versus time isotherms for several temperatures in the transformation region are shown in figure 2. All of these curves start at the equilibrium index (1.60500) for 600 °C (deformation point) at zero time. The change in index for each temperature was obtained from 600 to 421 °C within reasonable lengths of time. In addition, two approach curves were obtained for temperatures more than 150 °C below the critical point. One of these (351 °C) is shown plotted in figure 2, and it is noted that the change in index is still quite considerable. At a still lower temperature (250 °C) the change in index was still evident but its rate was too small for the time scale used $[(7 \pm 1) \times 10^{-5}$ in 20 hr] to be plotted in figure 2. As a result, it can be seen from these approach curves that the transformation region of a glass is very difficult to define. For practical experiments, the limits of the deformation point and a temperature of about

75 °C below the critical point will provide enough information in reasonable times for annealing studies. In comparison, for the same change in index for GeO₂ the temperature range is about 1.5 times that of the BSC glass [2] but the changes in index for GeO₂ were observed in about 1/4 of the time scale.

3.3. Equilibrium Index

Equilibrium indices were reached for several temperatures between 600 and 465 °C. These are shown plotted in figure 3. Unlike curves for most optical glasses this curve is not a straight line. It has a definite curvature much larger than any experimental uncertainty. The slope, $\frac{\partial N}{\partial T}$ decreases with increasing temperature. It is reasonable to assume that the expansion coefficient,

$$\alpha = 1/V \frac{\partial V}{\partial T} = C \frac{\partial N}{\partial T}, \quad (1)$$

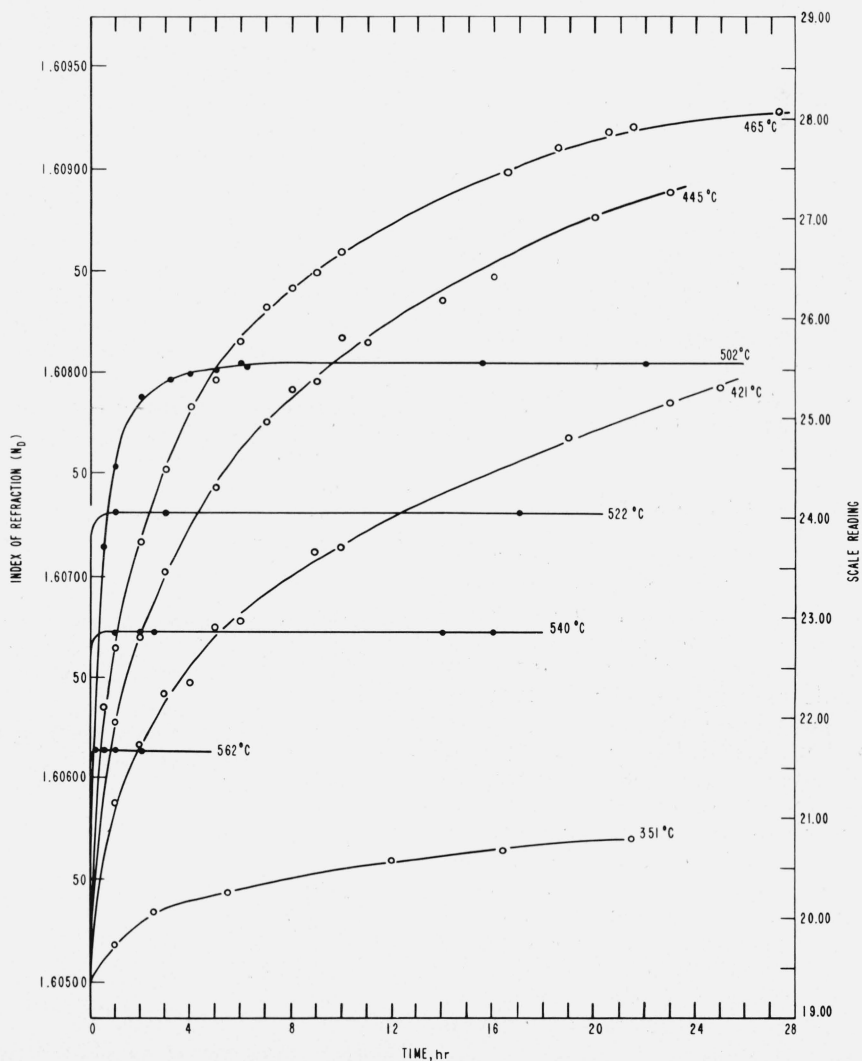


FIGURE 2. Index of refraction versus time isotherms for vitreous GeO₂.

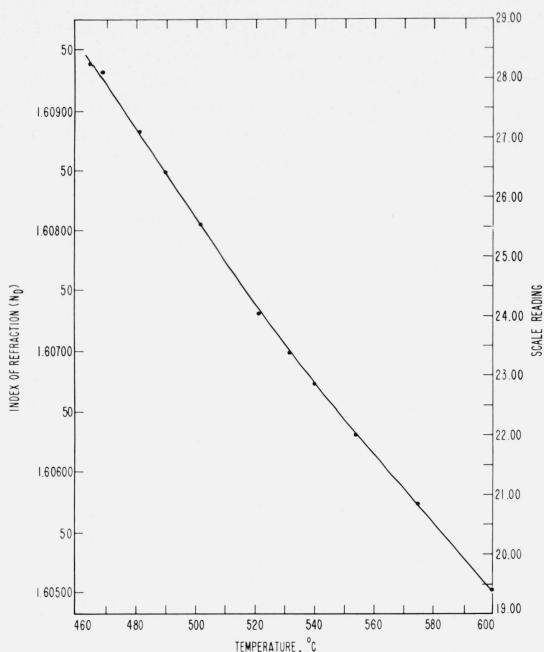


FIGURE 3. Equilibrium index versus temperature for vitreous GeO_2 .

in which V is the volume, and C is a constant. This leads to α decreasing with increasing temperatures for GeO_2 a behavior contrary to most liquids, but similar to B_2O_3 [14]. Macedo, Capps, and Litovitz [15] attributed this behavior in B_2O_3 , to the existence of two states separated by a step in energy, entropy, and volume. Unlike their work, because of the limited temperature range in GeO_2 , it is not possible to specify the two states in this case. Even so, the pronounced curvature in figure 3 strongly indicates the existence of a two state structure for GeO_2 .

3.4. Spectrum of Relaxation Times

In describing the relaxation curves [1] shown in figure 2 one has to consider both (a) the distribution of relaxation times as linear i.e., nonamplitude dependent and (b) a nonlinear relaxation process i.e., at any instant there is a distribution of relaxation times but at subsequent intervals each relaxation time changes with distance from equilibrium [16].

The existence of both a distribution of relaxation times and nonlinear effects make the calculation of the relaxation time spectrum very difficult if not impossible. In order to circumvent this problem the crossover technique [1, 2] will be used. The thermal history involved in the crossover can best be understood if one first understands the mathematical model used to represent the spectrum. The spectrum is assumed to be given by two relaxation mechanisms of equal strength, each having a single relaxation time. Thus the average index N is given as a function of time by the following relation

$$N = \frac{1}{2} [M_1(t) + M_2(t)] \quad (2)$$

where $M_i(t) = N_\infty + N_i \exp(-t/\tau_i)$, in which N_∞ is the equilibrium value of index; N_i , the initial deviation of index from N_∞ associated with mechanism i having relaxation times τ_i . This formulation can be thought of as describing the relaxation (change of volume) to a final equilibrium value following a change in temperature (analogous to an isothermal recovery function) in terms of two separate mechanisms, the first of which relaxes appreciably faster than the second. N_1 and N_2 are measures of the total relaxation undergone by the two separate mechanisms in reaching equilibrium. If the starting point is one of equilibrium [$M_1(0) = M_2(0)$], the two mechanisms will have to relax the same total amount $N_1 = N_2 = [N_\infty(T_1) - N_\infty(T_2)]$. However, when starting from a nonequilibrium approach curve, N_1 and N_2 will depend on the particular approach curve being followed. Figure 4 due to Macedo and Napolitano [1] shows schematically the time dependence of N , M_1 and M_2 at T_2 for a glass initially at equilibrium at T_1 , where $T_1 > T_2$. As the structure rearranges itself to the new equilibrium, M_1 will rise faster since it is associated with the shorter relaxation time τ_1 ; while M_2 will change more slowly. Thus, around the bend of the approach curve, there will be the largest difference between M_1 and M_2 in the glass. As time progresses, M_1 will reach its equilibrium value for T_2 first and stay there. From then on the spread between M_1 and M_2 narrows because the relaxation process associated with M_2 continuously approaches the same equilibrium but at a slower rate. Finally, when the structure is completely at the new equilibrium, the spread becomes zero, and one has again an equilibrium glass ($M_1 = M_2$).

The crossover experiment involves taking a glass having index, a , (see fig. 4) from the approach curve and introducing it into a furnace whose temperature is T_x . T_x is preselected such that the equilibrium index at T_x , $N_\infty(T_x)$, is equal to a . Thus at a crossover, a , the fast relaxation time (τ_1) corresponds to an index M_1 higher than the (average) measured value, N , and the slow relaxation time (τ_2) corresponds to an index M_2 lower than N .

If the index at the point of crossover, a , is equal to the equilibrium index at the crossover temperature T_x , then $N_2 = -N_1$. A prerequisite for a minimum in

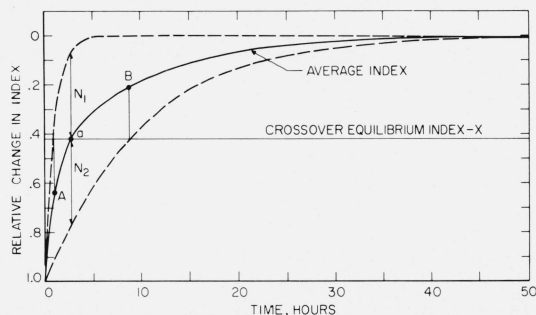


FIGURE 4. Illustration of two relaxation times (ref. [1]) represented by upper and lower dashed curves.

The average or measured index is given by solid line. The crossover equilibrium index (x) and the transfer point (a) are also shown.

the crossover experiment is that N_1 and N_2 have opposite signs. This is fulfilled when N has a value between A and B in figure 4. Figure 5, from Macedo and Napolitano [1] shows M_1 (the upper curve), M_2 (the lower curve) and N the solid line (calculated index). The agreement of the calculated curve with the actual experimental points for a borosilicate crown glass is seen to be good.

In the first crossover for GeO_2 , the glass was held to equilibrium at 600°C before quenching (see 2.3). The samples were then inserted into the furnace set at 421°C until their index approximately equaled N_∞ (519°C). At spaced time intervals, three samples were dropped from the furnace, one having an index equal to N_∞ (519°C), one with a higher index and one with a lower index. Finally, the temperature of the furnace is reset to 519°C , the three samples reinserted into the furnace, and successive index readings are then taken after short intervals in the furnace on each of the three samples. The results are plotted in figure 6. As a check for linearity all three curves were fitted with the same relaxation times $\tau_1 = 4.7$ min and $\tau_2 = 18.0$ min, but with different initial values (N_1 and N_2). The dip varied between 0.33 and 0.55 scale divisions as can be seen in figure 6. The fit was equally good for all three curves.

A more drastic check of linearity is to use relaxation times obtained from the crossover to calculate the approach curve. Figure 7 shows an approach curve from 538 to 523°C . The larger scatter in data is due to the fact that three different samples were used and as previously mentioned hydration was a problem. Since

$$N_1 = N_2 = N_\infty(523^\circ\text{C}) - N_\infty(538^\circ\text{C}) \quad (3)$$

and τ_1 and τ_2 were obtained from the crossover (519°C) there are no adjustable parameters in this curve.

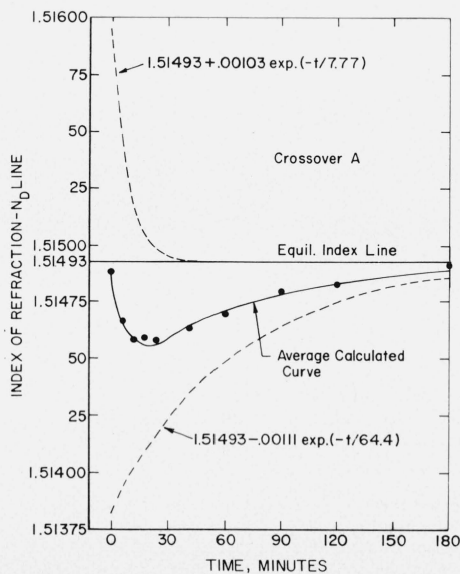


FIGURE 5. Crossover A for BSC glass (ref. [1], [2]) showing the average of the fast and the slow relaxation processes.

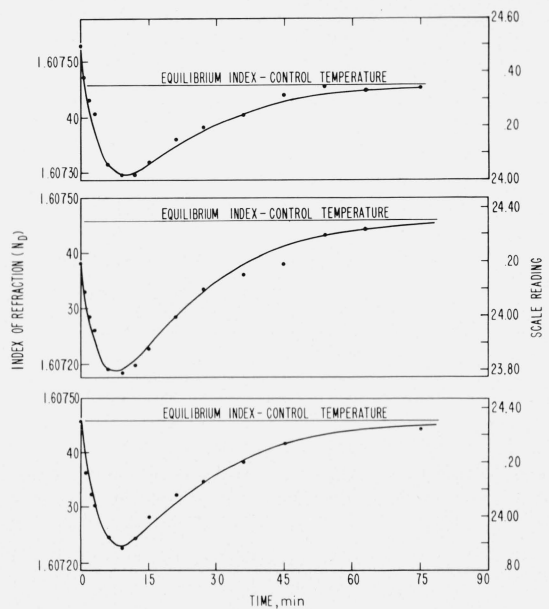


FIGURE 6. Index versus time for crossover having 421°C approach samples heat treated at 519°C .

Curves represent model with $\tau_1 = 4.7$ min and $\tau_2 = 18.0$ min are compared against experimental data.

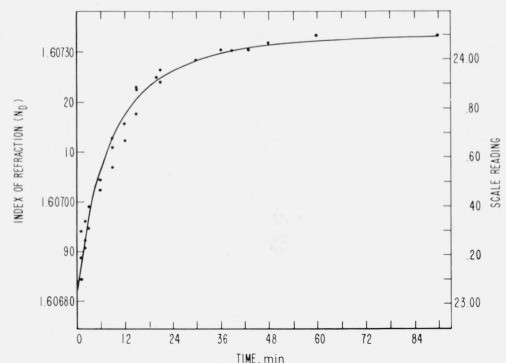


FIGURE 7. Approach curve for glass in equilibrium at 538°C to new equilibrium at 523°C .

Curve having same relaxation times as crossover in figure 6 is compared with experimental points obtained from three samples of glass.

This shows that the relaxation times were not changing with structural arrangements during the crossover, and that the spectrum obtained from the crossover does represent the full spectrum and not just the short and long times.

In addition two crossovers were measured at 489°C . One of these with an equilibrium value of index $[1.60500_{600^\circ\text{C}}]$ at zero time, 465°C approach temperature is shown at the top of figure 8 (curve B). The ratio of the relaxation time was much larger than that of 519°C where the ratio was 3.8. Since the dip was so shallow it was decided to repeat this experiment selecting two temperatures which would give a deeper dip. Using an equilibrium value of index ($1.60745_{518^\circ\text{C}}$) at zero time, 428°C approach temperature and the same 489°C crossover temperature, the dip was 44

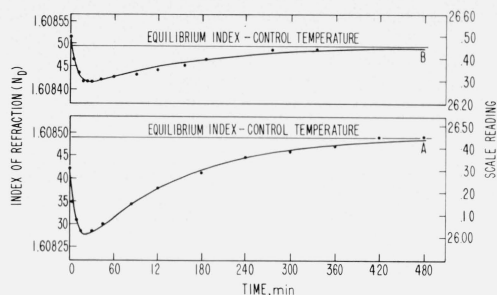


FIGURE 8. Index versus time for crossover A and B having equilibrium temperature 489 °C.

Both curves have the same relaxation times ($\tau_1=9.3$ min and $\tau_2=130$ min). Sample A came from a 428 °C approach, while samples B came from a 465 °C approach.

scale divisions (curve A) compared with the earlier 15 scale divisions (curve B). Both crossovers could be fitted with the same relaxation times of $\tau_1=9.3$ min and $\tau_2=130$ min. Thus the ratio of the relaxation times τ_2/τ_1 at 489 °C, 14, was about 3.7 times larger than at 519 °C.

3.5. Viscosity

Low temperature viscosities on the GeO_2 glass were measured by the fiber elongation method [17]. Measurements were made with two types of fiber, flame-drawn and fibers drawn directly from the melt. Since no differences were found in the viscosity values using

each type of fiber, all subsequent measurements were made with the flame-drawn fibers because of the ease of fabrication. The measured values are given in table 1 as well as the stabilization or annealing times and melt numbers. Since there was no trend between different melts, they were not distinguished in subsequent treatments.

Figure 9 shows both the data from this work and those of Fontana and Plummer [3] below 600 °C plotted versus reciprocal absolute temperature. In general the data from both laboratories agree with each other. The scatter in the data is about the same for each set of data. Even so, the least squares fit of each set of data gave considerably different activation energies shown in table 2. The solid curve represents the combined fit, which is practically identical to the NBS curve, and has a lower slope than the short dashed line (Fontana and Plummer data below 600 °C fitted to the Arrhenius curve). This probably occurs because Fontana and Plummer have only two data points below 535 °C while NBS has 10 points, one of which was stabilized for 138 hr (481.3 °C).

Fontana and Plummer report that all the data above ~650 °C (below 5×10^{10} P) is fitted by an Arrhenius curve with an activation energy of 64.2 kcal/mol (1 cal=4.184J). This curve is also plotted in figure 9 as the long dashed line. Even though the viscosity has unquestionably departed from the Arrhenius curve it is in the "near" Arrhenius region.

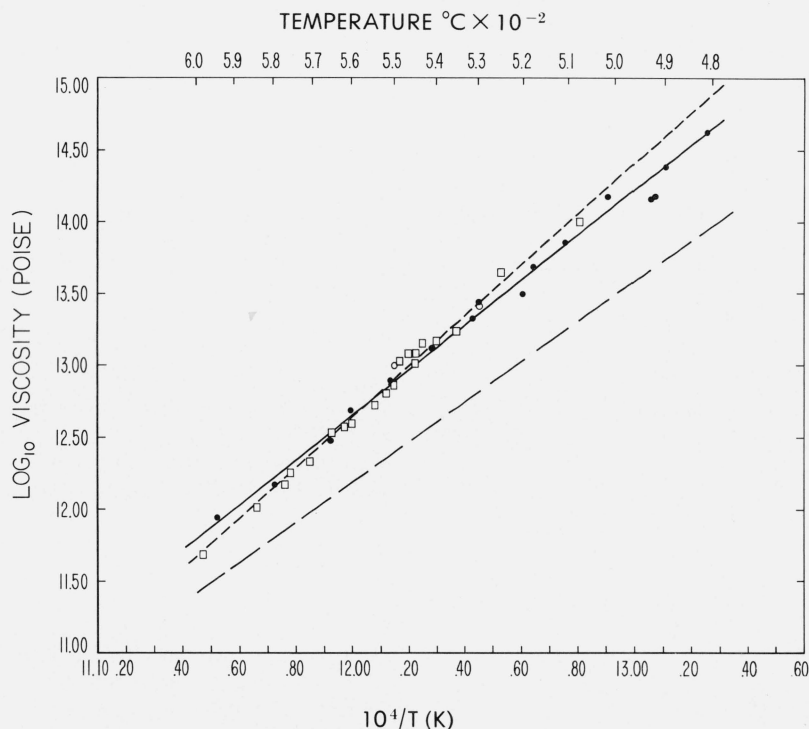


FIGURE 9. Arrhenius plot of viscosity.

- , F & P ref. [3].
 - , Flame drawn fibers.
 - , Fiber drawn from crucible
- } from present work.
- - - , least squares fit to F & P data.
 - , least squares fit of combined data - NBS and F & P.
 - , least squares fit-extrapolation of high temperature Arrhenius fit of F & P data.

TABLE 1. Viscosity data for germania glass by the fiber elongation method

Melt No.	Temp. °C	η	Time held
3	481.3	14.615	138 hr
2	489.7	14.382	8 hr
3	492.0	14.169	23 hr
2	492.9	14.152	71 hr
3	501.9	14.167	17 hr
3	511.1	13.854	17 hr
3	518.3	13.681	2 hr
2	520.1	13.490	3 hr
1	^a 530	13.408	16 hr
1	530	13.437	21 hr
2	531.3	13.323	18 hr
3	540.9	13.113	16 hr
1	^a 550.2	12.995	7 hr
3	551.1	12.887	1 hr
3	560.7	12.685	1 hr
2	566.1	12.475	1 hr
1	579.3	12.167	1 hr
3	594.8	11.939	1 hr
1	633.4	10.996	45 min

^a Fibers drawn from crucible.

TABLE 2. Coefficients of data from table 1 and reference 3, plotted in figure 9, from the equation $\ln \eta = A + E_\eta/RT$

	A	E_η kcal/mol	ΔE_η ^a kcal/mol
Fontana and Plummer.....	-8.646	81.7	1.7
NBS.....	-5.739	70.6	1.8
Combined.....	-6.178	72.3	1.5

^a Standard error of E_η .

4. Discussion

4.1. Comparison of Volume and Shear Relaxation Times

The shear viscosity, η , is given by [18]

$$\eta = G_\infty \int_0^\infty \tau_{sg}(\tau_s) d\tau_s = G_\infty \bar{\tau}_s \quad (4)$$

where G_∞ is the modulus of shear rigidity. Thus, the temperature dependence of η is either equal to that of $\bar{\tau}_s$ or a little larger depending on the behavior of G_∞ . First, one can compare the temperature dependence of the average volume relaxation times $\bar{\tau}_{PT}$ as measured by annealing, with the shear viscosity. The $\bar{\tau}_{PT}$ was calculated according to

$$\bar{\tau}_{PT} = \frac{1}{2} (\tau_1 + \tau_2), \quad (5)$$

remembering our assumption that both mechanisms were weighted equally. The average time ($\bar{\tau}_{PT}$) was 11.4 min at 419 °C and 69.6 min at 489 °C. The ratio is 6.1 as compared with the ratio for the shear viscosity 6.2 for these same two temperatures. This discrepancy is well within the experimental uncertainty of both experiments.

Next the absolute magnitude of the shear and volume relaxation time should be compared. Since the annealing experiments were carried out at atmospheric pressure and constant temperature the volume relaxation time reported above is isobaric isothermal. Because

most of the data of this type are obtained by acoustical techniques [19], the proper thermal condition to compare is isochoric, adiabatic ($\bar{\tau}_{vs}$). Unfortunately we do not have the necessary data to perform the transformation (see ref [1]), but we should expect that the ratio of $\bar{\tau}_{PT}/\bar{\tau}_s$ to be larger than $\bar{\tau}_{vs}/\bar{\tau}_s$ because $\bar{\tau}_{PT}/\bar{\tau}_{vs} > 1$ [1]. The average shear relaxation time was calculated by eq (4), using the G_∞ of Strakna et al. [20], and our viscosity data. For 519 °C, $\bar{\tau}_s = 3.7$ min and the ratio, $\bar{\tau}_{PT}/\bar{\tau}_s$ was 3.1, a value in good agreement with other liquids [19].

4.2. Temperature Dependence of Spectrum of Relaxation Times

Unlike BSC glass, the GeO_2 spectrum is temperature dependent. Between 489 and 519 °C the ratio of τ_2/τ_1 changes from 14 to 3.8. The equal weight given to the two relaxation times which was originally assumed is required to fit the data in figures 6, 7, and 8. Thus, the symmetry of the spectrum is characteristic of the data and not a mathematical artifact. Symmetric spectrums can also be represented in terms of Gaussian distributions. Figure 10 shows the equivalent Gaussian distribution of relaxation times

$$g_\tau(\tau) = \frac{b}{\sqrt{\pi}} \exp(b \ln \tau/\tau')^2 \quad (6)$$

where the most probable relaxation time, τ' , has been set to

$$\tau' = \sqrt{\tau_1 \cdot \tau_2}. \quad (7)$$

The width, b , has been chosen such that the frequency dependence of the real part of the compressibility most closely matches the function obtained from

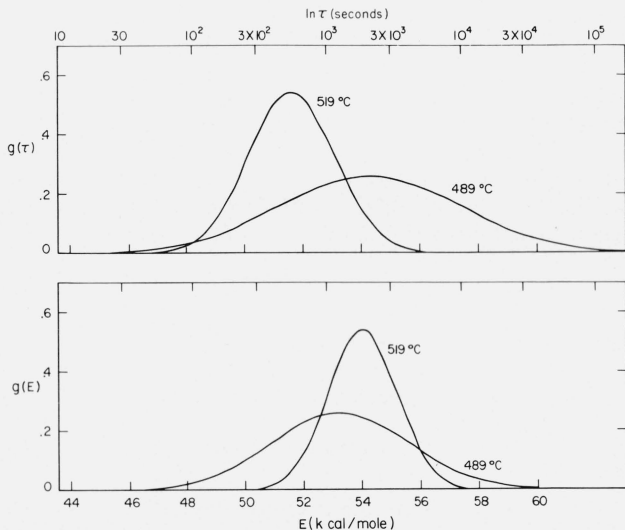


FIGURE 10. Plot of the relaxation time spectrum and the activation energy distribution.

Note that since A in eq 10 is unknown the position of the peaks in the activation energy distribution is arbitrary.

$\tau_1 - \tau_2$ calculation [5]. The broadening of the spectrum resembles that observed for B_2O_3 [7]. In B_2O_3 the spectrum is single where the temperature dependence of the viscosity is Arrhenius and it broadens as the viscosity departs from the Arrhenius curve. Thus, a probable explanation for a temperature dependent spectrum is that the measurements were made in the transition zone between Arrhenius and non-Arrhenius region. In fact at 489 °C the viscosity is only a factor of 3.5 above the Arrhenius curve.

The two relaxation time model provides us with four different activation energies. A comparison of the activation energy E_a , associated with the average relaxation time with that for shear viscosity in this temperature range was made and found to be in good agreement. These activation energies are respectively $E_a = 73$ kcal/mol and $E_\eta = 72.3$ kcal/mol. The activation energy E_2 associated with τ_2 , the long relaxation time, is 79 kcal/mol which is larger than E_η as would be expected. On the other hand the activation energy E_1 , associated with τ_1 the short relaxation time, is 28 kcal/mol. The surprising fact here is that E_1 is so much smaller than E_a . In fact it is much smaller than the Arrhenius activation energy for shear viscosity. This confirms the surprising conclusion obtained for B_2O_3 [7] that the cause of the non-Arrhenius region is not a higher average activation but rather the appearance of a distribution of energies some of which are larger than \bar{E} . It should be emphasized at this point that not only have higher activation energies appeared but also lower ones.

For better comparison with the B_2O_3 work, Gaussian distributions of activation energies $g_E(E)$ were calculated in the following manner: By using Eyring's rate equation [21]

$$\tau = A \exp(E/RT) \quad (8)$$

where A is a constant; E , the activation energy; T , the temperature in K; and R , the gas constant, and assuming that A is the same constant for all the relaxation spectrum one can calculate the distribution of activation free energy. This assumption is consistent with the viscosity theories [22, 23, 24] which will be discussed below. The fractional number of molecules which relaxes with relaxation time τ_i between $\ln \tau_i - 1/2 d \ln \tau$ and $\ln \tau_i + 1/2 d \ln \tau$ is

$$g_\tau(\tau_i) d \ln \tau = g_E(E_i) dE \quad (9)$$

where $g_E(E_i) dE$ is the fractional number of molecules with activation free energy between $E_i - 1/2 dE$ and $E_i + 1/2 dE$. The activation free energy E_i is given by

$$E_i = RT \ln(\tau_i/A) \quad (10)$$

where A (seconds) is an unknown constant since we do not have data in the Arrhenius region. It was chosen such that the curves superimposed for better comparison. Figure 10 also shows $g_E(E)$ for both temperatures. Note that $g_E(E)$ is a Gaussian in E not in $\ln E$. Thus, the average and most probable values coincide.

The distributions shown in figure 10 for GeO_2 agree with the B_2O_3 work.

We have found in GeO_2 supporting evidence that the departure from the Arrhenius curve for viscosity is caused by the appearance of a distribution of relaxation times, and, further, that the associated distribution of activation energies has not only higher activation energies but also lower. The present theories which predict non-Arrhenius behavior are typified by the work of Ree, Ree, and Eyring [22], Adam and Gibbs [23], and Davies and Matheson [24]. These theories picture the molecules as being relatively free at high temperatures in the Arrhenius region, and connect the appearance of non-Arrhenius behavior with some increase in cooperation between molecules, or a loss in certain degrees of freedom as the temperature is lowered. This leads to an increase in apparent activation energies but it is *not* clear how any of these theories can lead to the presence of *smaller* activation energies.

5. Summary

The glass transition region of GeO_2 has been studied by, first, measuring thermal expansion ($7.7 \times 10^{-6}/^\circ C$) in a slowly heated sample (deformation point 600 °C, critical point 505 °C); second, measuring shear viscosity by fiber elongation (from 10^{11} to 6×10^{14} P); and third, measuring the effect of annealing from index of refraction-time isotherms and the crossover technique. The viscosity values were found to be in good agreement with those of Fontana and Plummer. In view of the more extensive low temperature data in this report a lower and more precise value of the activation energy in the annealing region ($E_\eta = 72.3$ kcal/mol) was obtained. The equilibrium index was not linear with temperature. The negative departure of the slope indicates that the structure of GeO_2 can probably be fitted by a two state model similar to B_2O_3 .

The previously reported [1] two relaxation time model was used to analyze the annealing experiment data for GeO_2 , and proved to be equally good as in BSC glass. This ruled out the original contention that the two-relaxation model might be due to a two-liquid immiscibility in the BSC glass. Since these experiments were designed with "a priori" knowledge of the mathematical model, very clear evidence of its applicability was demonstrated by comparing a crossover with an approach curve.

Unlike most materials GeO_2 has a spectrum of relaxation times which is temperature dependent in the annealing range. This occurs because the viscosity values are only just departing from Arrhenius behavior, and the origin of this departure is the appearance of a distribution of relaxation times. The temperature dependence of the spectrum was analyzed in terms of a distribution of activation energies. A conclusion of this study is that, similar to B_2O_3 , activation energies smaller than the activation energy present in the Arrhenius region appear at low temperatures.

We thank J. M. Nivert for preparing the samples; E. G. Hawkins for making the fiber viscosity measurements and E. H. Hamilton (retired) for making the expansion run above room temperature.

6. References

- [1] Macedo, P. B., and Napolitano, A., Effects of a distribution of volume relaxation times in the annealing of BSC glass, *J. Res. NBS* **71A** (Phys. and Chem.) No. 3, 231-238 (1967).
- [2] Spinner, S., and Napolitano, A., Further studies in the annealing of a borosilicate glass, *J. Res. NBS* **70A** (Phys. and Chem.) No. 2, 147-152 (1965).
- [3] Fontana, E. H., and Plummer, W. A., A Study of viscosity-temperature relationships in the GeO_2 and SiO_2 systems, *Phys. Chem. Glasses* **7**, No. 4, 139-146 (1966).
- [4] Kurkjan, C. R., and Douglas, R. W., Viscosity of glasses in the system $\text{Na}_2\text{O}-\text{GeO}_2$, *Phys. Chem. Glasses* **1**, No. 1, 19-25 (1960).
- [5] Macedo, P. B., and Litovitz, T. A., Ultrasonic viscous relaxation in molten boron trioxide, *Phys. Chem. Glasses* **6**, No. 3, 69-80 (1965).
- [6] Litovitz, T. A., and McDuffie, G., Comparison of Dielectric and mechanical relaxation in associated liquids, *J. Chem. Phys.* **39**, 729 (1963).
- [7] Tauke, J., Litovitz, T. A., and Macedo, P. B., Viscous relaxation and non-Arrhenius behavior in B_2O_3 , *J. Am. Ceram. Soc.* **51**, 158-163 (1968).
- [8] Litovitz, T. A., and Macedo, P. B., Ultrasonic Relaxation, Viscosity and Free Volume in Molten Glasses, "Phys. of Non-Crystalline Solids", Delft Conference 1964 (North Holland Publishing Co., Amsterdam, pp. 220-228 (1965)).
- [9] Grauer, O. W., An improved refractometer, *NBS Tech. News Bull.* **37** (9) 135 (1953); **38** (4) 63 (1954).
- [10] Saunders, J. B., Improved interferometric procedure with application to expansion measurements, *J. Res. NBS* **23**, 179-195 (1939) RP1227.
- [11] Mackenzie, J. D., Density and expansivity of vitreous germania, *J. Am. Ceram. Soc.* **42**, 310 (1959).
- [12] Dennis, L. M., and Laubengayer, A. W., Germanium XVII. Fused germanium dioxide and some germanium glasses, *J. Phys. Chem.* **30**, No. 11, 1510-1526 (1926).
- [13] Spinner, S., and Cleek, G. W., Temperature dependence of Young's modulus of vitreous germania and silica, *J. Appl. Phys.* **31**, No. 8, 1407-1410 (1960).
- [14] Napolitano, A., Macedo, P. B., and Hawkins, E. G., Viscosity and density of boron trioxide, *J. Amer. Ceram. Soc.* **48**, [12] 613-616 (1965).
- [15] Macedo, P. B., Capps, W., and Litovitz, T. A., Two-State Model for the Free Volume of Vitreous B_2O_3 , *J. Chem. Phys.* **44**, 3357-64 (1966).
- [16] Condon, E. U., "Comments on—The annealing of flat glass", *The Glass Industry* **33**, 307, 322-3 (1952).
- [17] Napolitano, A., and Hawkins, E. G., Viscosity of a standard soda-lime-silica glass, *J. Res. NBS* **68A** (Phys. and Chem.), No. 5, 439-448 (1964).
- [18] Herzfeld, K., and Litovitz, T. A., Absorption and Dispersion of Ultrasonic Waves (Academic Press, New York and London 1959).
- [19] Litovitz, T. A., and Davis, C. M., *Physical Acoustics*, Vol. **II**, Ch. 5 (Academic Press, New York and London, 1965).
- [20] Strakna, R. E., and Savage, H. T., Ultrasonic relaxation loss in SiO_2 , GeO_2 , B_2O_3 , and As_2O_3 glass, *J. Appl. Phys.* **35**, [5] 1445-50 (1964).
- [21] Glasstone, S. N., Laidler, K., and Eyring, A., *The Theory of Rate Processes* (McGraw-Hill Book Company, Inc., New York, 1941).
- [22] Ree, T. S., Ree, T., and Eyring, A., Significant liquid structure theory IX. Properties of dense gases and liquids, *Proc. N.A.S.*, **48**, 501 (1962).
- [23] Adam, G., and Gibbs, J. H., On the temperature dependence of cooperative relaxation properties in glass-forming liquids, *J. Chem. Phys.* **43**, 139 (1965).
- [24] Davies, D. B., and Matheson, A. J., Influence of molecular rotation of the viscosity of liquids, *J. Chem. Phys.* **45**, 1000 (1966).

(Paper 72A4-509)